Acoust. Sci. & Tech. **33**, 1 (2012)

PAPER

Tidal current measurement in the Kurushima Strait by the reciprocal sound transmission method

Yudi Adityawarman[1], Arata Kaneko[1,*], Naokazu Taniguchi[1], Hidemi Mutsuda[1], Katsuaki Komai[1], Xinyu Guo[2] and Noriaki Gohda[3]

[1]*Graduate School of Engineering, Hiroshima University, 1–4–1 Kagamiyama, Higashi-Hiroshima, 739–8527 Japan*
[2]*Center for Marine Environmental Studies, Ehime University, 2–5 Bunkyo-cho, Matsuyama, 790–8577 Japan*
[3]*Aqua Environmental Monitoring Limited Liability Partnership, 12–2 Aobadai, Mihara, 723–0047 Japan*

(*Received 13 May 2011, Accepted for publication 18 September 2011*)

Abstract: The tidal current in the Kurushima Strait of the Seto Inland Sea, Japan was successfully measured during July–August 2009 (36 days) among the three acoustic stations (KR4, KR5 and KR6), located on both sides of the strait. The travel time differences for the two sound transmission lines KR4–KR5 and KR4–KR6 are converted into the range-averaged currents along the transmission lines. The hourly mean of the range-averaged currents varied in the range from −31.1 to 53.8 cm/s for the KR4–KR5 and in the range from −45.4 to 48.7 cm/s for the KR4–KR6 with the error bars of 5.0 cm/s and 6.6 cm/s, respectively. The hourly mean along-line currents are further transformed into the geophysical coordinates with the variation range from −99.1 to 91.6 cm/s and the mean current of −6.6 cm/s for the eastward component V_E, and that of (−54.2–31.5) cm/s and the mean current of −7.6 cm/s for the northward component V_N. The cross-line volume transport varied in the range of (−17.928 to +17.569) × 10^4 m^3/s, resulting in the mean westward transport of 0.727 × 10^4 m^3/s. This mean transport reaches a significant level over the error bar of 0.474 × 10^4 m^3/s.

Keywords: Tidal current, Volume transport, Reciprocal sound transmission method, Kurushima Strait, Seto Inland Sea

PACS number: 43.30.Pc [doi:10.1250/ast.33.45]

1. INTRODUCTION

The Kurushima Strait is a narrow passage of width about 1 km, located at the central part of the Seto Inland Sea and separates the Aki-nada and Hiuchi-nada (Fig. 1). The strait is the most important shipping route not only in the inner Japan, but also between Korea and China, and Japan, and then always crowded by traffic ships. Furthermore the strong, complicated tidal currents occur especially around the central parts of the strait, surrounded with small islands. These environmental conditions have frequently caused the traffic accident such as ship wrecks and collisions.

The tidal current measurement in the strait has been limited due to heavy shipping. Especially the current measurement from fixed-position type sensors such as bottom-mounted and subsurface-moored currentmeters is prohibited in the ship traffic route at the central part of the strait by the Japan Coast Guard (JCG). The half-month measurement by the surface drifters was performed in 1956 by the JCG. The predicted values of surface current are now opened to the public because they provide important information which makes the operation of traffic ships safe (http://www1.kaiho.mlit.go.jp/KAN6/2_kaisyo/tidal-current/tidalc_forecast.html).

However, the near surface current is not good enough to assess environmental issues like the volume exchange of water (volume transport) between the neighboring seas (Aki-nada and Hiuchi-nada). For the environmental protection and management, the volume transport of water is preferable to be measured in addition to the surface current.

The first fixed point observation of tidal currents in the Kurushima Strait was carried out during the half month, using the four moored JCG buoys, deployed during the

*e-mail: akaneko@hiroshima-u.ac.jp

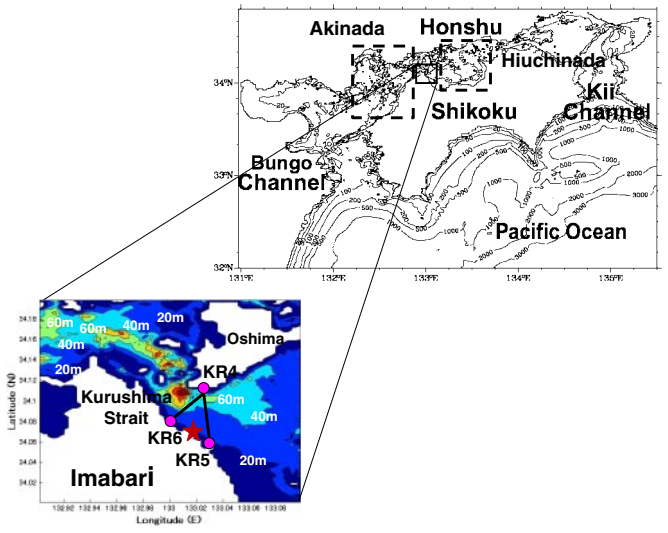

Fig. 1 Location map of the experimental site and the surrounding region with the bathymetric chart. KR4, KR5 and KR6 are the acoustic stations. The solid lines connecting the stations show the travelling sound transmission lines. The tide gauge station is shown with the star mark. The whole region of the Seto Inland Sea is shown in a shrinkage scale at upper right of the figure.

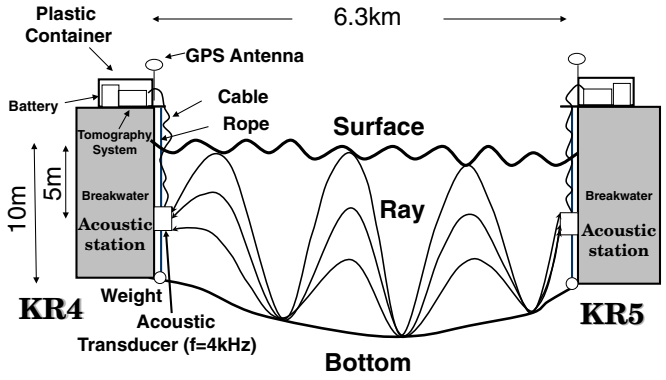

Fig. 2 Schematic diagram of the tomography system for the reciprocal sound transmission experiment, placed on the breakwater of the fisheries ports (KR4 and KR6) and trade port (KR5).

dredge work for the extension of ship route [1]. The time variation of tidal currents was roughly understood by this experiment although less accuracy is caused by the application of rotor-type velocimeters in the strong tidal current and no data across the strait were acquired. The advanced current measurement in the Kurushima Strait was carried out by the shipboard ADCP in 1993. However, the observational lines did not cross the central part of the strait from a safety viewpoint and the repeat ADCP surveys continued only for several hours [2,3]. The tidal current in the Kurushima Strait was simulated by the 3D coastal sea circulation model with a sea level forcing at the open boundaries. However, the results were not validated by the direct observation of current although the vortex generation behind the islands was reasonably simulated [4]. The half-month current measurement was performed by two bottom-mounted upward-looking ADCPs, located in the specified positions displaced from the traffic route [5]. The data at the central part were supplemented by the 10-hour repeat operation of the shipboard ADCP. However, the results did not reach a level to estimate the volume transport through the strait. The data sampling in the vertical cross section across the strait is insufficient both horizontally and vertically to estimate the volume transport. It is, thus, concluded that the volume transport through the Kurushima Strait has never been measured with satisfactory accuracy.

The coastal acoustic tomography system (CATS), which has been developed by Hiroshima University as an application of deep-sea acoustic tomography [6], and well operated in the coastal seas around Japan [7], is applicable to the Kurushima Strait as well, located on the eastern side of Aki-nada [12]. The current measurement can be done without disturbing the shipping from the sound transmission and reception stations (acoustic stations), located on both sides of the strait.

The CATS is here applied to measure the tidal current in the Kurushima Strait and to estimate the volume transport through the strait. This is the first application of CATS to transport variations in straits with heavy shipping.

2. EXPERIMENT

A reciprocal sound transmission experiment was carried out among three acoustic stations (KR4, KR5 and KR6) during July–August 2009 (36 days) to measure the tidal current in the Kurushima Strait of the Seto Inland Sea (Fig. 1). The horizontal distance is 6.32 km for the station pair KR4–KR5 and 4.13 km for the station pair KR4–KR6. The reciprocal sound transmission data were obtained between both the station pairs. The sound transmission for the station pair KR5–KR6 was prohibited by the protruded artificial shoreline. The floor depth for the mean sea level is 13 m at KR4 and increased rapidly to 57 m at 1.5 km away from KR4. The floor depth is gradually decreased from 44 m at 2.5 km to 10 m at KR5. For KR4–KR6 the floor depth forms a more simple profile such that it is increased to about 60 m at the middle from about 10 m at the edge. A coastal acoustic tomography system (CATS) was placed on the breakwater which protects the fisheries ports (KR4 and KR6) and the trade port (KR5). The 4 kHz acoustic transducer was suspended down by a rope in water 5 m below the surface in front of the offshore side of the breakwater and connected to the CATS via a cable (Fig. 2). The CATSs were operated by the 12 V rechargeable battery and sound was transmitted with 24 V power, using two 12 V batteries in a serial connection.

The transducer (ITC 2002A) is of the broad-band type with central frequency 4 kHz and band width 1.5 kHz. The transducer works not only for sound transmission, but also for sound reception. The source level of the broad-band transducer is 192 dB re 1 μPa at 1 m and the average power consumption is 480 W during the sound transmission. In this experiment, the transmitted signal was phase-modulated by the 10th order M sequence to increase the signal-to-noise ratio (SNR) of received signals by $20 \log \sqrt{2^{10} - 1} = 30$ dB. This gain of SNR is attained by the cross-correlation of received signals with the M sequence, used in the transmission. The 3 cycles per digit (Q-value) was selected to transmit the phase-modulated sound from the broad-band transducer. The transmission of 4 kHz sound in the 3 cycles per digit requires the frequency band-width 4 kHz/3 = 1.3 kHz which the present transducer satisfies. Notice that the smaller Q-values are selectable for the transducer of the wider frequency range. The time resolution for multi-path arrivals t_r, defined as one-digit width of M sequence, is given 0.75 ms. One period (0.76725 s) of 4 kHz sound, phase-modulated by the M sequence, was released every 4 minutes at the synchronized timing from KR4, KR5 and KR6. The 4-min interval data were smoothed through an hourly moving average to increase the signal-to-noise ratio (SNR) of received signals by $20 \log \sqrt{16} = 12$ dB.

The received signals are sampled with a vertical resolution bit of 10 at the frequency of 8 kHz and cross correlated with the M sequence. The travel times are determined at a maximum peak point in each of the correlation waveforms, obtained every 4 minutes. The range-average velocity V_m and sound speed C_m between two acoustic stations may be estimated from the travel time difference Δt and mean travel time t_m, respectively, in the following formulation [13]:

$$t_1 = \frac{L}{C_m + V_m}, \tag{1}$$

$$t_2 = \frac{L}{C_m - V_m}, \tag{2}$$

where L denotes the station-to-station distance, and the t_1 and t_2 denote the travel times from station T1 to T2 and from station T2 to T1, respectively. By solving the coupled Eqs. (1) and (2), we obtain

$$V_m = \frac{L}{2t_1 t_2} \Delta t, \tag{3}$$

$$C_m = \frac{L}{t_1 t_2} t_m, \tag{4}$$

where $\Delta t = t_2 - t_1$ and $t_m = (t_1 + t_2)/2$.

The CTD casts were performed at a 0.5 km interval on July 15 along the sound transmission line KR4–KR5. The results were used as data not only to know the profiles of temperature, salinity and sound speed, but also to execute the range-independent ray tracing simulation of travelling sound. The temperature and salinity are well homogenized due to the strong tidal current that always occurs in the strait. As a result, the sound speed is monotonically increased with the pressure, forming a constant gradient. The result of ray simulation serves to know the depth range at which rays travel in a vertical section, and is shown in Fig. 3. Sound travels, spanning almost all the vertical sections except the trough, placed at 1.0–1.5 km from KR4 and the near-bottom region at 3.5–5.0 km from it.

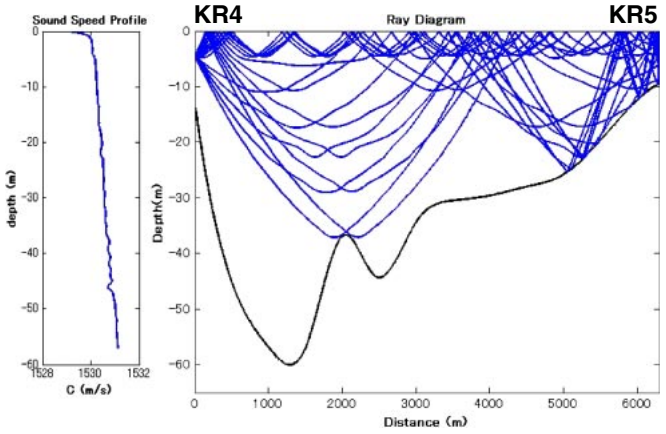

Fig. 3 Result of the range-independent ray simulation for the launch angles at an increment of 0.2° between −2.0° and +2.0°, performed by using the CTD data at the maximum depth (1 km from KR4) on July 15. The vertical profiles of sound speed (C) are shown at left of the figure.

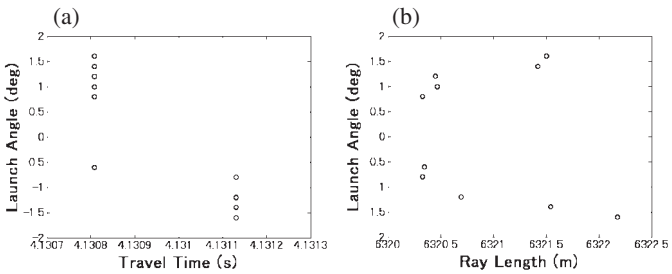

Fig. 4 (a) Acoustic travel times and (b) ray lengths for all the rays, plotted against the launch angles.

The acoustic travel times and ray lengths for the rays with launch angles at an increment of 0.2° between −2.0° and +2.0° are plotted against the launch angles at the source in Figs. 4(a) and 4(b), respectively. The travel time data are separated into two groups, bounded at −0.5° of launch angle and centered at 4.13081 s to 4.13112 s while the ray length draws a rough parabolic curve. However the variation range of travel time difference of 0.30 ms is smaller than $t_r = 0.75$ ms (one-digit length of the M sequence), the time resolution for multi-path arrivals. The

time resolution of $t_r = 0.75$ ms for multi-path arrivals determines the resolution of velocity measurement. As a result, the multi-path arrivals cannot be resolved in the received signals, so all the arrival rays cooperate to construct a broad arrival peak. This property provides a big advantage in estimating the vertical-section average current from the travel time for the biggest, broad arrival peak. The ray lengths distribute in the range from 6,320.3 m to 6,322.2 m.

We shall here refer the resolution of velocity measurement, related to the time resolution of $t_r = 0.75$ ms for multi-path arrivals. By substituting t_r into Δt in Eq. (3), the velocity resolution is determined 13.9 cm/s. The velocity resolution reduces to 5.6 cm/s when t_r is replaced by the simulated variation range of travel time difference (0.30 ms).

3. RESULTS AND DISCUSSION

The correlation waveforms of acoustic signals traveling from KR5 to KR4 during 9:00 of July 7 to 9:00 of July 8 are shown in Fig. 5 with the stack diagrams as a typical case together with those from KR4 to KR5. In this figure, the transmission time on the vertical axis is elapsed upward. Furthermore the stack diagrams for 5:00–6:00 of July 8 are shown in a magnified scale at right of the figures. There is a big peak in each of the correlation waveforms to show the arrival of travelling sound. The travel times are determined at top of the peak. Only the peak points with the signal-to-noise ratios SNR > 7 are used as significant arrival signals in estimate of range-averaged current. The frequent occurrence of data lacking are visible in the stack diagrams. The hull of crowded traffic ships and their associated bubble-included wakes which frequently pass the Kurushima Strait make a barrier to the travelling sound and cause the data lacking.

The range-averaged current is calculated for periods when the reciprocal data are successfully acquired and permit the estimation of travel time difference. The range-averaged currents V5 and V6 for the station pairs KR4–KR5 and KR4–KR6 are shown with the time plot in Figs. 6(a) and 6(b). Both the 4-min interval original data and the hourly mean data are shown in the figures. The hourly mean current varies in the range from −31.1 to 53.8 cm/s for the KR4–KR5 and from −45.4 to 48.7 cm/s for the KR4–KR6. The mean for two fortnightly periods (27.32 days) is 7.7 cm/s for the KR4–KR5 and 10.2 cm/s for the KR4–KR6. The semi-diurnal and fortnightly variations of tides are more clearly seen for the KR4–KR5 data than for the KR4–KR6 data. For KR4–KR5 the tidal variation is diminished due to the large period of data lacking during July 27–31. The root mean squares difference (RMSD) between the original data and hourly mean data is 5.0 cm/s for KR4–KR5 and 6.6 cm/s for KR4–KR6.

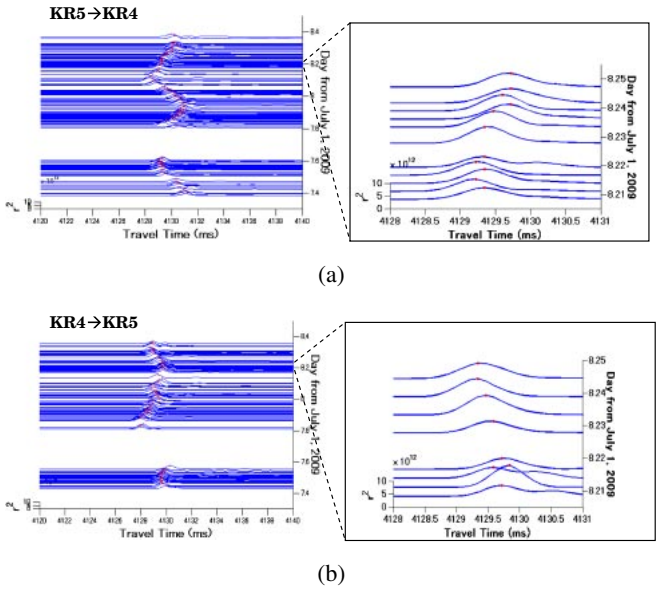

Fig. 5 Stack diagrams of the correlation waveforms, obtained at KR4 (upper panel) and KR5 (lower panel) for the station pair KR4–KR5 during 9:00 of July 7–9:00 of July 8. The diagrams for 5:00–6:00 of July 8 are shown in a magnified scale at right of the figures. The biggest peaks are located with the red dot on each correlation waveform. The correlation functions are labeled with r.

The RMSD may be regarded as an upper limit of errors for hourly current measurement because the errors are included in the short-term variability [14]. The upper limit of error is here called the error bar. The error bar is estimated 5.0 cm/s for KR4–KR5 and 6.6 cm/s for KR4–KR6. It is here worth noting that the error bars (5.0 cm/s and 6.6 cm/s) are nearly equal to the resolution of velocity measurement (5.6 cm/s), implying that almost all errors are produced by the velocity resolution.

The along-line currents (V_5, V_6) for (KR4–KR5, KR4–KR6) are converted into the east and north components of current (V_E, V_N) by the following formulae (Fig. 7):

$$V_E = \frac{V_5 \cos\theta_6 - V_6 \cos\theta_5}{\sin\theta_5 \cos\theta_6 - \cos\theta_5 \sin\theta_6}, \tag{5}$$

$$V_N = \frac{-V_5 \sin\theta_6 + V_6 \sin\theta_5}{\sin\theta_5 \cos\theta_6 - \cos\theta_5 \sin\theta_6}, \tag{6}$$

where θ_5 and θ_6 denote the angles of the transmission lines KR4–KR5 and KR4–KR6 measured clockwise from the north, and are put as $\theta_5 = 180.2°$ and $\theta_6 = 219.6°$, respectively. Notice that the velocity data for the two transmission lines located at different places are necessary to evaluate the vector components of current (V_E, V_N), and Eqs. (5) and (6) can be obtained under the assumption that (V_E, V_N) does not change between the two transmission lines KR4–KR5 and KR4–KR6. As another explanation, (V_E, V_N) may be considered as currents at the middle of KR4–KR5 and KR4–KR6.

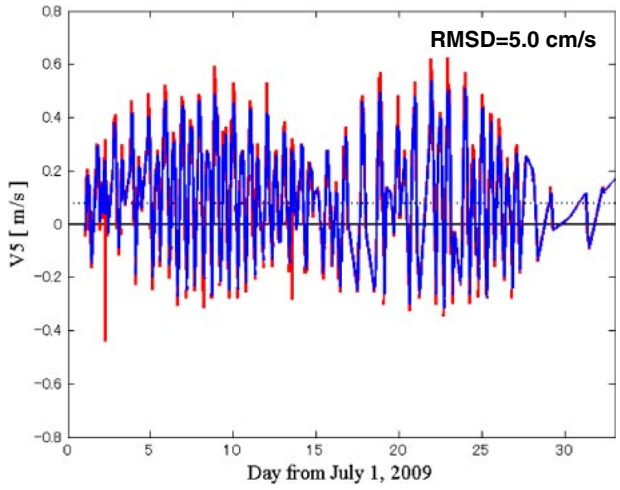

(a)

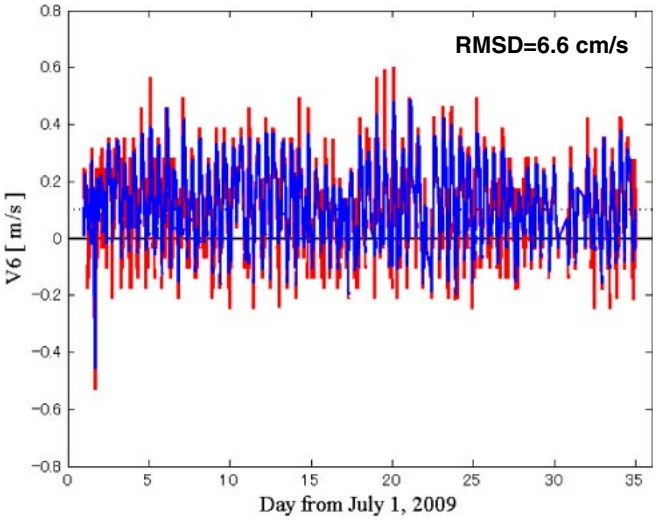

(b)

Fig. 6 Time plots of the range-averaged currents (V_5 and V_6) obtained along the transmission lines (a) KR4–KR5 and (b) KR4–KR6. The 4-min interval original data and hourly mean data are shown in the red and blue solid lines, respectively. The dashed line indicates the mean for two fortnightly periods (27.32 days). The RMSD between both the data are presented at upper right of both the figures.

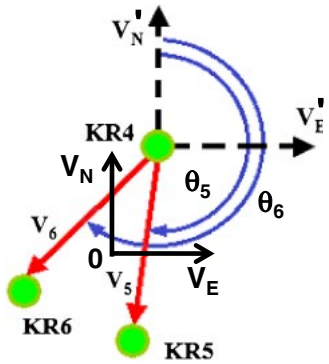

Fig. 7 Sketch of the coordinate transformation from the along-line components (V_5, V_6) into the east-north components (V_E, V_N). The origin of the coordinate frame (V_E, V_N) is placed at the center of KR4–KR5 and KR4–KR6, and that of the shifted coordinate frame (V_E', V_N') is placed at KR4 parallel to (V_E, V_N) to measure the direction of transmission line.

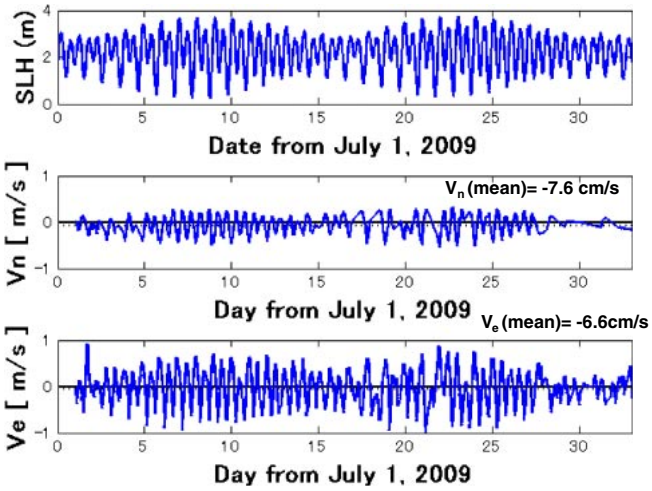

Fig. 8 Time plots of the hourly mean eastward current V_E (middle panel) and northward current V_N (lower panel) for the entire observational period. The 27.32 hours mean currents are shown with the horizontal, dashed lines, and their values are put at upper right of each figure. The sea level data at the tide gauge station IMABARI of the JCG are presented at upper panel of the figure.

The (V_E, V_N) currents for the hourly mean data are shown in Fig. 8 with the time plots. The V_E and V_N for the hourly mean current vary in the range from −99.1 to 91.6 cm/s and from −54.2 to 31.5 cm/s, respectively. The average of the hourly mean data for two fortnightly periods (27.32 days) is (−6.6, −7.6) cm/s for the (east, north) component and thus the resultant current is directed southwestward.

The volume transport through the strait is calculated from a product of the range-averaged current and vertical cross section area. The transport is calculated for both the transmission lines KR4–KR5 and KR4–KR6. The range-averaged current (V_p) in the directions perpendicular to KR4–KR5 and KR4–KR6 is calculated from (V_E, V_N), obeying the following formulae:

$$V_p = V_E \cos\theta_t - V_N \sin\theta_t, \tag{7}$$

where $\theta_t = \theta_5 - 180^\circ$ ($\theta_5 = 180.2^\circ$) for KR4–KR5 and $\theta_t = \theta_6 - 180^\circ$ ($\theta_6 = 219.6^\circ$) for KR4–KR6. By putting the vertical cross section area into A, the volume transport (Q) across KR4–KR5 and KR4–KR6 may be expressed by

$$Q = V_m \times A, \tag{8}$$

where $A = 214{,}164\,\mathrm{m}^2$ for KR4–KR5 and $A = 161{,}325\,\mathrm{m}^2$ for KR4–KR6.

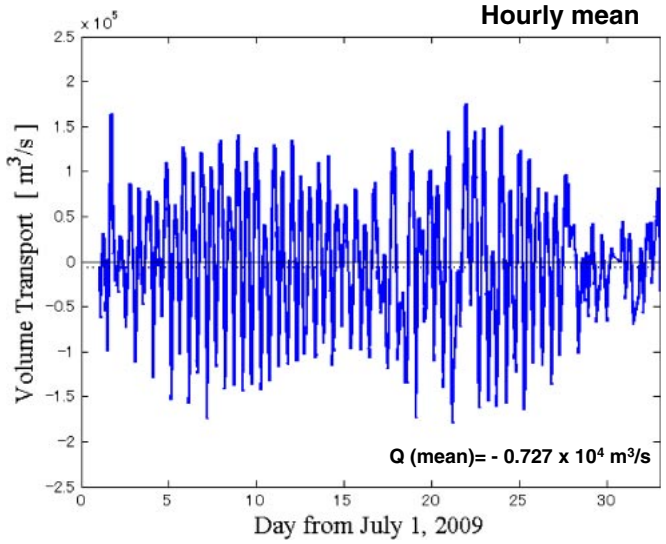

Fig. 9 Time plots of the hourly mean cross-line volume transport for the entire observational period. The 27.32 hours mean transport for the hourly data is shown with the horizontal, dashed lines, and its value is put at lower right of the figure.

The volume transport through the strait may be estimated as the average of transports across KR4–KR5 and KR4–KR6, and is shown in Fig. 9 with the time plots for the hourly mean data. The hourly mean data vary in the range of $(-17.928$ to $+17.569) \times 10^4\,\mathrm{m^3/s}$, resulting in the mean westward transport of $0.727 \times 10^4\,\mathrm{m^3/s}$.

The westward mean transport may be associated with the counter-clockwise tidal vortex, generated on the south-eastern side of the Oshima island during the eastward tidal current phase [3,4]. This vortex is released southwestward along the southern coast of the Oshima with the growth of westward tidal current, forming the westward residual transport. The eastward mean current in Aki-nada seems to be erased by the stronger local effect due to vortex generation in the Kurushima Strait. The connectivity of mean current from the former to latter requires further study.

4. SUMMARY

The tidal current in the Kurushima Strait is announced at a real time from the JCG to the traffic ships for preventing ship accidents. However, the opened data are predicted on the basis of near surface tidal current data acquired at the central part of the strait, making the most priority for the announcement to traffic ships. The whole vertical cross section average of tidal current through the strait is difficult to be estimated from the data, acquired at the near surface layer of the central part. Therefore the along-strait volume transport has never been correctly estimated which play a critical role in water exchange and environmental dependency between Aki-nada and Hiuchi-nada.

The reciprocal sound transmission experiment was carried out for the two pairs of acoustic stations (KR4–KR5 and KR4–KR6), located on the both sides of the Kurushima Strait. The range-averaged currents are estimated along the two transmission lines KR4–KR5 and KR4–KR6, using the travel time difference data. The average current is close to the current averaged over the vertical cross section because the acoustic rays traveling between the acoustic stations span almost all parts of the vertical section. The average current for two fortnightly periods (27.32 days) is 7.7 cm/s for the KR4–KR5 and 10.2 cm/s for the KR4–KR6. The error bars are 5.0 cm/s and 6.6 cm/s smaller than the corresponding average currents.

The two along-line currents are transformed into the east and north components of current (V_E, V_N). The variation range from -99.1 to 91.6 cm/s for V_E is considerably larger than that from -54.2 to 31.5 cm/s for V_N. V_E stronger than V_N is caused by that the strait is bounded by the 4th biggest Japanese main island (Shikoku) and Oshima island on the southern and northern sides, respectively. The 27.32-day mean current $(-6.6, -7.6)$ cm/s (10.1 cm/s in magnitude) for the (east, north) component is directed southwestward with a significant level over the error bar (5.8 cm/s on average).

The volume transport through the strait is estimated by taking a product of the hourly mean cross-line current and vertical cross section area. The volume transport makes a variation range of $(-17.928$ to $+17.569) \times 10^4\,\mathrm{m^3/s}$, resulting in the mean westward volume transport of $0.727 \times 10^4\,\mathrm{m^3/s}$. This westward mean transport reaches a significant level over the error bar because the error bars of current (5.0 cm/s and 6.6 cm/s for KR4–KR5 and KR4–KR6, respectively) cooperate to produce the error bar of transport ($0.474 \times 10^4\,\mathrm{m^3/s}$).

The reciprocal sound transmission method provides an innovational technique to measure the tidal current variations in straits with crowded shipping like the Kurushima Strait. The volume transport through the strait is successfully estimated over the error level, but more accurate result may be obtained by increasing the station-to-station distance.

ACKNOWLEDGEMENTS

We thank Mr. Hiromitsu Ichiki for his contribution in observation and data analysis. Dr. Yoshio Takasugi is greatly acknowledged for the kindest support in the instrumentation. This study is supported by a grant from the Japan Society for the Promotion of Science.

REFERENCES

[1] H. Takeoka and A. Higuchi, "Current measurement in the Kurushima Strait," *Note Coastal Sea Stud.*, **18**(1), pp. 29–36 (1980) (in Japanese).
[2] M. Tada, S. Susami, T. Toyota, N. Chimoto, T. Fujiwara and

A. Hoshika, "Characteristics of tidal currents around the south east part of the Kurushima Kaikyo, the Seto Inland Sea," *Mem. Yuge Natl. Coll. Marit. Technol.*, **15**, 15–19 (1993) (in Japanese with English abstract and figure captions).

[3] M. Tada, S. Susami, T. Toyota, N. Chimoto, S. Mizui, J. Seto, Y. Takasugi and T. Fujiwara, "Characteristics of tidal currents around the south east part of the Kurushima Kaikyo, the Seto Inland Sea (II)," *Mem. Yuge Natl. Coll. Marit. Technol.*, **16**, 27–31 (1994) (in Japanese with English abstract and figure captions).

[4] H. Mutsuda, Y. Doi and Y. Ichii, "Seal level distribution and the 3D structures of tidal current in the Kurushima Strait using coastal circulation model," *J. Coastal Eng. JSCE*, **49**, 376–380 (2002) (in Japanese).

[5] A. Okabayashi, Y. Takahashi, H. Shibaki and T. Takao, "Analysis of the characteristics of tidal current at Kurushima Strait — Field observations and numerical simulation of 3D-flow," *J. Coastal Eng. JSCE*, **55**, 416–420 (2008) (in Japanese with English abstract).

[6] W. Munk, P. F. Worcestor and C. Wunsch, *Ocean Acoustic Tomography* (Cambridge University Press, Cambridge, 1995).

[7] J.-H. Park and A. Kaneko, "Assimilation of coastal acoustic tomography data into a barotropic ocean model," *Geophys. Res. Lett.*, **27**, 3373–3376 (2000).

[8] K. Yamaguchi, J. Lin, A. Kaneko, T. Yamamoto, N. Gohda, H.-Q. Nguyen and H. Zheng, "A continuous mapping of tidal current structures in the Kanmon Strait," *J. Oceanogr.*, **61**, 283–294 (2005).

[9] J. Lin, A. Kaneko, N. Gohda and K. Yamaguchi, "Accurate imaging and prediction of Kanmon Strait tidal current structures by the coastal acoustic tomography data," *Geophys. Res. Lett.*, **32**, L14607. doi:10.1029/2005GL022914 (2005).

[10] A. Kaneko, K. Yamaguchi, T. Yamamoto, N. Gohda, H. Zheng, F. Syamsudin, J. Lin, H. Nguyen, M. Matsuyama, H. Hachiya and N. Hashimoto, "A coastal acoustic tomography experiment in Tokyo Bay," *Acta Oceanol. Sin.*, **24**, 86–94 (2005).

[11] H. Nguyen, A. Kaneko, J. Lin, K. Yamaguchi, N. Gohda and Y. Takasugi, "Acoustic measurement of multi sub-tidal internal modes generated in Hiroshima Bay, Japan," *IEEE J. Oceanic Eng.*, **34**, 103–112 (2009).

[12] Y. Adityawarman, A. Kaneko, K. Nakano, N. Taniguchi, X. Guo and N. Gohda, "Reciprocal sound transmission experiment of throughflow and temperature variations across the central part of the Seto Inland Sea, Japan," *J. Oceanogr.*, **67**, 173–182, doi:10.1007/s10872-011-0016-5 (2011).

[13] A. Kaneko, N. Gohda, H. Zheng, T. Takano, H. Yamaoka, J.-H. Park and K. Yamguchi, "Coastal acoustic tomography," *Umi-No-Kenkyu*, **12**, 1–19 (2003) (in Japanese with English abstract and figure captions).

[14] H. Yamaoka, A. Kaneko, J.-H. Park, H. Zheng, N. Gohda, T. Takano, X.-H. Zhu and Y. Takasugi, "Coastal acoustic tomography system and its field application," *IEEE J. Oceanic Eng.*, **27**, 283–295 (2002).